ELSEVIER

Journal of Arid Environments 69 (2007) 1–14

Journal of Arid Environments

www.elsevier.com/locate/jaridenv

An object-based image analysis approach for determining fractional cover of senescent and green vegetation with digital plot photography ☆

A.S. Laliberte*, A. Rango, J.E. Herrick, Ed L. Fredrickson, L. Burkett

USDA-Agricultural Research Service, Jornada Experimental Range, New Mexico State University, Las Cruces, NM 88003, USA

Received 10 July 2006; received in revised form 18 August 2006; accepted 26 August 2006
Available online 3 November 2006

Abstract

Research into automatic image processing of digital plot photography has increased in recent years. However, in most studies only overall vegetation cover is estimated. In arid regions of the southwestern US, grass cover is typically a mixture of green and senescent plant material and it is important to be able to quantify both types of vegetation. Our objectives were to develop an image analysis approach for estimating fractional cover of green and senescent vegetation using very high-resolution ground photography, and to compare image-based estimates with line-point-intercept (LPI) measures. We acquired ground photography for 50 plots using an eight megapixel digital camera. The images were transformed from the RGB (red, green, blue) color space to the IHS (intensity, hue, saturation) color space. We used an object-based image analysis approach to classify the images into soil, shadow, green vegetation, and senescent vegetation. Shadow and soil were effectively masked out by using the intensity and saturation bands, and a nearest neighbor classification was used to separate green and senescent vegetation using intensity, hue and saturation as well as visible bands. Correlation coefficients between LPI- and image-based estimates for green and senescent vegetation were 0.88 and 0.95 respectively. Image analysis underestimated total and

☆ Mention of trade names or commercial products in this publication is solely for the purpose of providing specific information and does not imply recommendation or endorsement by the US Department of Agriculture.

*Corresponding author. Tel.: +1 505 646 4144; fax: +1 505 646 5889.

E-mail addresses: alaliber@nmsu.edu (A.S. Laliberte), arango@nmsu.edu (A. Rango), jherrick@nmsu.edu (J.E. Herrick), efredric@nmsu.edu (E.L. Fredrickson), lburkett@nmsu.edu (L. Burkett).

0140-1963/$ - see front matter Published by Elsevier Ltd.
doi:10.1016/j.jaridenv.2006.08.016

senescent vegetation by approximately 5%. The object-based image-processing approach is less labor and time intensive than the LPI method, is a viable alternative to ground-based methods, and has the potential to be incorporated into rangeland monitoring protocols.
Published by Elsevier Ltd.

Keywords: Rangeland vegetation; Rangeland monitoring; Very high-resolution images; Object-based image analysis

1. Introduction

Research focused on image analysis techniques for measuring vegetation cover and/or bare soil from digital ground photography is becoming increasingly common (Bennett et al., 2000; Louhaichi et al., 2001; Richardson et al., 2001; Booth et al., 2005), although methods developed by these efforts have yet to be widely adopted (Booth et al., 2006). Most studies using image processing only estimate total vegetation cover of the plot. In order to assess rangeland condition and trend, and to determine the nutritional value of vegetation for livestock and wildlife grazing, rangeland managers need to be able to measure fractional cover values for bare soil and vegetation, as well as fractional composition of green (live) and senescent (dead) vegetation. Ground-based plot estimates are a common tool for assessing rangeland vegetation cover (Herrick et al., 2005), but are time consuming and labor intensive (Herrick et al., 2006). Image-based methods can be faster once fully developed, and they have the added advantage that photos can be acquired quickly for different times to assess vegetation dynamics for monitoring purposes. In addition, photos are easily archived; thus, conserving maximal data for future change analyses.

At the USDA-ARS Jornada Experimental Range in southern New Mexico, ongoing research is aimed at relating ground-based observations to remotely sensed data at various scales (Laliberte et al., 2004, in press). Our goal for this study was to develop an image analysis approach for quantifying vegetation characteristics from very high-resolution digital photography. Specific objectives were to quantify bare soil and vegetation cover, to separate and quantify green and senescent vegetation, and to compare cover estimates from image analysis with those obtained from line-point-intercept (LPI) data collected on the ground.

In arid rangelands, green and senescent plant materials are often intermixed and difficult to differentiate, especially with digital imagery having only three bands (red, green, blue or RGB) and lacking a near infrared band. Band inter-correlation is relatively high in the RGB space, but is reduced when images are transformed to the intensity-hue-saturation (IHS) space. The IHS color representation is based on a color sphere rather than a cube as in the RGB space (Jensen, 2005). Intensity relates to brightness and is represented as the vertical axis of the sphere. Hue is the dominant wavelength of the color and is represented as the circumference on the sphere. Saturation is defined as the relative purity of the color and is represented as the sphere's radius. The IHS model separates the intensity component from the color information, while hue and saturation components relate to how humans perceive color (Jensen, 2005).

Some authors have reported increased accuracy in vegetation analysis using digital images with IHS transformations rather than the original RGB bands. For example, Tang

et al. (2000) used a genetic algorithm for segmenting very high-resolution video images i n the IHS image space for detecting weeds in crops. Hemming and Rath (2001) segmented and classified digital images using spectral and spatial features in IHS space. IHS transformations also were used by Ewing and Horton (1999) to estimate wheat canopy cover and by Karcher and Richardson (2003) for quantifying turf grass cover.

Digital image analysis of plot photography traditionally was performed using pixel-based image analysis, whereby each pixel's digital number is assessed individually. Another option is object-based image analysis, whereby pixels are aggregated in a first step (segmentation) into objects that are homogenous with regard to spatial or spectral characteristics (Ryherd and Woodcock, 1996). Homogeneity in this case refers to smaller within-object than between-object variance. In a second step, those objects rather than single pixels are classified. Object-based image analysis is an effective tool for classification of high-resolution satellite imagery (Herold et al., 2003; Thomas et al., 2003; Lennartz and Congalton, 2004; Laliberte et al., 2004), but to our knowledge has not been applied with ground plot photography in rangelands. In ecological studies, object-based image analysis is advantageous, because this approach allows for detection of landscape patches, which offers insight into ecological processes (Hay et al., 2002; Burnett and Blaschke, 2003). Plot photography is an effective tool for detecting changes in patch structure at a scale that is relevant to many soil and ecological processes, including wind erosion (Okin et al., 2006). It is also an appropriate scale for vegetation classification (Booth et al., 2005) and analyses of changes in the spatial pattern of vegetation (Bestelmeyer et al., 2006).

2. Methods

2.1. Study Area

Our research was conducted at the Jornada Experimental Range (JER; approx. elevation 1200 m), which is located approximately 40 km northeast of Las Cruces, New Mexico in the northern Chihuahuan Desert. Average monthly maximum temperatures range from 13 °C in January to 36 °C in June, and mean annual precipitation is 241 mm of which more than 50% falls during July, August and September. Historically, most of this area was a desert grassland, but shrub encroachment by honey mesquite (*Prosopis glandulosa* Torr.), creosotebush (*Larrea tridentata* (Sess. & Moc. ex DC) Cov.), and tarbush (*Flourensia cernua* DC.) has led to a conversion of much of the area to desert scrub (Gibbens et al., 2005). Our study was conducted in a 1200 ha pasture, which consists of most vegetation communities found within the Jornada del Muerto basin floor. Dominant grass species included black grama (*Bouteloua eriopoda* (Torrey) Torrey), tobosa (*Pleuraphis mutica* Buckley), dropseed (*Sporobolus* spp.), threeawn (*Aristida* spp.), and burrograss (*Scleropogon brevifolius* Phil.). Dominant shrub species included honey mesquite, four-wing saltbush (*Atriplex canescens* (Pursh) Nutt.), soap-tree yucca (*Yucca elata* Engleman.), mormon tea (*Ephedra torreyana* (Wats.), and broom snakeweed (*Gutierrezia sarothrae* (Pursh) Britt. & Rusby). While black grama and tobosa tend to occur in pure stands, dropseed and threeawn are often intermixed.

2.2. LPI sampling and ground photography acquisition

A stratified random field sampling approach was used to locate 50 plots within five dominant vegetation communities: black grama, tobosa, mixed grasses, broom snakeweed, and bare soil. Communities dominated by large shrubs were not included in this study. We used an eight megapixel Canon Powershot Pro 1 digital camera fixed to an aluminum pole to acquire a ground photo for each plot from a height of 2.8 m. The resulting images had a size of 3264×2448 pixels, covered a $2.5\,m \times 3.5\,m$ plot and had an approximate ground resolution (pixel size) of 1 mm. Images were acquired between 9:30 am and 3:30 pm to minimize the influence of shadow. Ground sampling was performed using LPI techniques described by Herrick et al. (2005), using four, 2.5 m lines located 0.25 m from the edge of the plot and 1 m apart. Points were sampled every 10 cm, for a total of 104 points per plot. The contact area of the point of the pin was approximately 1 mm square. Foliar cover was calculated for soil, green vegetation, senescent vegetation, and by species for each line. Data from those lines were averaged for the plot. We used only the first (top) intercept that touched vegetation and/or soil, thus accurately representing the aerial view in the digital image.

2.3. Image segmentation and analysis

The images were imported into Erdas Imagine 8.7 (Leica Geosystems GIS and Mapping, 2003) and converted from RGB to IHS space. Subsequent analysis of RGB and IHS images was conducted using eCognition, an object-based image analysis program (Definiens, 2003). In this approach, an image is segmented into homogeneous areas based on three parameters: scale, color (spectral information), and shape. Color and shape can be weighted from zero to one. Within the shape setting, smoothness or compactness can be defined and weighted from zero to one. The scale parameter is unit-less and controls the relative size of image objects (polygon or segment), with a larger scale parameter resulting in larger image objects. The images were segmented at a scale parameter of 5, and color/shape and smoothness/compactness settings of 0.9/0.1 and 0.5/0.5, respectively.

Analysis in eCognition can be conducted using either a nearest-neighbor classification based on selected samples (similar to a supervised classification in pixel-based analysis), or with membership functions, representing a rule-base classification. For example, the class bare ground may be described as all values in band X greater than a, where a is the mean value of all pixels representing an image object. A general rule in eCognition is that membership functions are appropriate if a class is relatively easy to separate from another and can be described with one or a few rules. Nearest-neighbor classification is more appropriate when classes are more difficult to separate from each other, because this approach is better suited for evaluating correlation between object features and for describing a multidimensional feature space (Definiens, 2003). For a nearest-neighbor classification, suitable samples have to be selected for each class.

In this case, we chose a combination of membership functions and nearest-neighbor classification and used a masking approach, which allowed for classifying easily identifiable classes first and more difficult ones later. We classified *Shadow* first by determining its threshold value in the intensity band using "Feature View", a tool that allows for visualizing a feature (image band or ratio of bands) and determining threshold values for classification. (Note: in this paper, senescent vegetation, green vegetation, soil,

and shadow are in Italics when referring to class names in eCognition.) All other image objects were grouped into the *Not Shadow* class by using a membership function with inverted similarity to the class *Shadow*. The inverted similarity is a rule describing all image objects that are "not in the class shadow". All objects in the *Not Shadow* class were classified into either *Soil* by determining the soil threshold values in the saturation and hue bands, or into *Vegetation* (which equaled "not in the class soil") by using a membership function with inverted similarity to the class *Soil*. At this point, only *Vegetation* remained to be classified and confusion between *Senescent Vegetation* and *Soil* was therefore eliminated. *Green Vegetation* and *Senescent Vegetation* were classified by using a nearest neighbor approach using 10–15 sample objects for each class (Fig. 1).

In eCognition's nearest neighbor classification, samples are selected, the image is classified, and in a subsequent step, wrongly assigned objects or unclassified objects are assigned to the correct classes. This step can be repeated if needed to stabilize the classification. The choice of input features was determined both visually and using the "Feature Space Optimization" (FSO) tool. This tool evaluates the distance in feature space between the samples of classes, and selects layer combinations that result in the best class separation distance. We used the FSO tool on six test images. The choice of features was consistent across the test images; therefore, we selected the 13 selected features for all 50 images. Those features included the mean and ratio of each input band (red, green, blue, intensity, hue, saturation), and the maximum difference. The mean of an input band in eCognition is calculated as the mean value of all pixels forming an image object. The ratio is calculated as the band's mean value for an image object divided by the sum of all band mean values. The maximum difference is the maximum value minus the minimum value of an image object.

Part of the analysis was automated by using a protocol, similar to a macro, which segmented the image, loaded the class hierarchy (selected classes), and classified the image initially. Subsequent fine-tuning of the classification was necessary for adjustment of the intensity, saturation and hue values for the *Shadow* and *Soil* classes, as well as for sample selection. For all images, percent cover values for the classes *Shadow*, *Soil*, *Green Vegetation*, and *Senescent Vegetation* were summarized in eCognition. Correlation and regression analysis was used to assess the strength of the relationship between image- and LPI-based estimates.

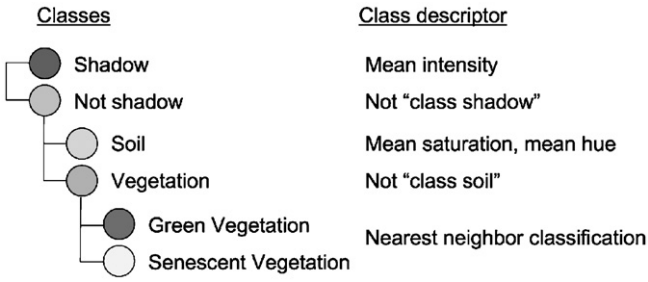

Fig. 1. Classes and class descriptors used in the image analysis program eCognition. A masking approach was used. *Shadow*, *Not Shadow*, *Soil*, and *Vegetation* were classified with membership functions using specific rules. *Green Vegetation* and *Senescent Vegetation* were classified with the nearest-neighbor approach using samples.

3. Results

3.1. Image analysis

Image transformation from RGB to IHS space was an effective tool for classification in this study. The intensity band clearly differentiated *Shadow* from *Non-Shadow* in the first step of the image analysis. The hue and saturation bands were equally effective in separating *Soil* and *Vegetation* in the second step. In plots dominated by black grama and/or tobosa grasses, the saturation band alone was sufficient for separating *Soil* and *Vegetation*, while in plots with broom snakeweed, the combination of the saturation and hue bands was more effective. In plots with very sparse vegetation, hue alone was effective for separating *Soil* and *Vegetation*. Except for a few outliers, the mean values for intensity, hue, and saturation used for thresholding had a relatively narrow range (Table 1). One outlier for saturation (0.34) occurred in a plot with 94% vegetation cover and another outlier for saturation (0.06) occurred in a plot with a large amount of shadow. Due to the narrow range of values for intensity, hue and saturation, we were able to use the timesaving protocol that resulted in an initial classification and only required subsequent fine-tuning of the mean values.

Shadow cover ranged from 0.2% to 22.2% with a mean of 6.5%, although 55% of images had less than 6% shadow. Shadow is always problematic in very high-resolution images, because it occurs both on the soil surface as well as within the vegetation canopy. However, shadow was easily classified, and was placed in its own class in this analysis. Further classification of the vegetation class into *Green Vegetation* and *Senescent Vegetation* was performed with samples and nearest neighbor classification. Image objects representing green and senescent vegetation were chosen as training samples for the nearest neighbor classification algorithm. In most images, the smallest overlaps in feature space for samples chosen for green and senescent vegetation existed in the mean hue, ratio hue and mean red bands (Fig. 2). This figure is a typical illustration of the separation between green and senescent vegetation in feature space, even though each image had different values and ranges in feature space. Given the relatively large overlap in feature space for *Green Vegetation* and *Senescent Vegetation*, the initial masking of shadow and soil areas was an

Table 1
Statistics for mean intensity, hue and saturation values used to threshold shadow, soil and vegetation classes in eCognition for 50 ground photos

Statistic	Mean intensity	Mean hue	Mean saturation
Average	0.26	145	0.16
Standard deviation	0.04	2	0.05
Median	0.26	146	0.16
Mode	0.23	147	0.17
Minimum	0.13	140	0.06
Maximum	0.34	150	0.34
n	50	36	39

Intensity, hue and saturation are referred to as means because pixels are averaged for image objects. Mean intensity was used to separate *Shadow* and *Non-Shadow* classes, hue and/or saturation were used to separate *Soil* and *Vegetation* classes. Statistics (except *n*) are expressed in digital numbers (unit-less).

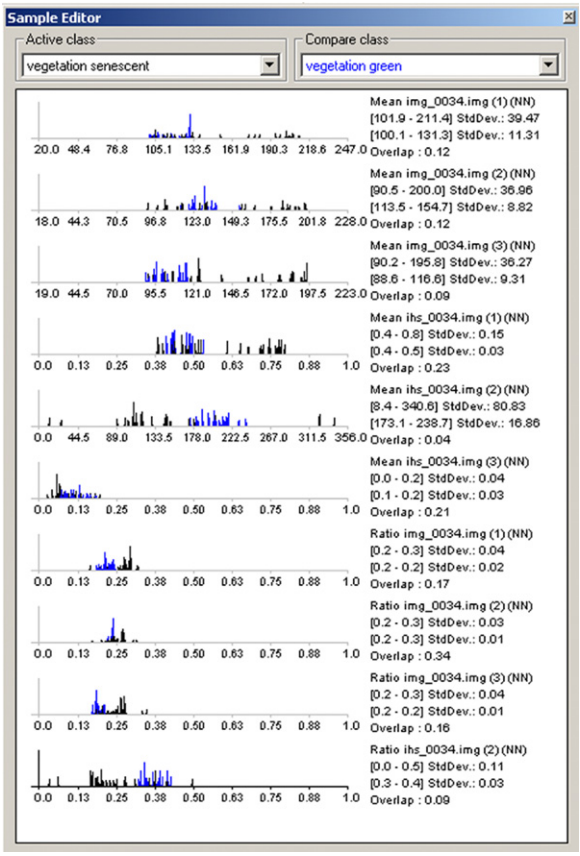

Fig. 2. Comparison of histograms for selected samples (image objects) of *Senescent Vegetation* (in black) and *Green Vegetation* (in blue). Each column in the histogram represents the sample's value for each feature. Features shown are (from top): mean blue, mean green, mean red, mean intensity, mean hue, mean saturation, ratio blue, ratio green, ratio red, ratio hue.

appropriate step. Without this approach, added confusion between senescent vegetation and bright soil would have occurred.

Despite encountering plots of varying vegetation types and total vegetation cover ranging from 0% to 94% (with a mean of 36.6%)(values from LPI data), our image classification approach was effective for all conditions. The red, green and blue bands were highly correlated which did not allow for much differentiation between green and senescent vegetation, while the intensity, hue and saturation bands were more effective for this purpose (Fig. 3).

3.2. Comparison of LPI and image analysis

Correlations between LPI-based and image-based cover estimates for total vegetation cover, soil, green and senescent vegetation were relatively high (Table 2, Fig. 4). The best correlations were obtained for total vegetation cover and senescent vegetation, while green vegetation had the lowest correlation coefficient of 0.88. Compared to the LPI estimates,

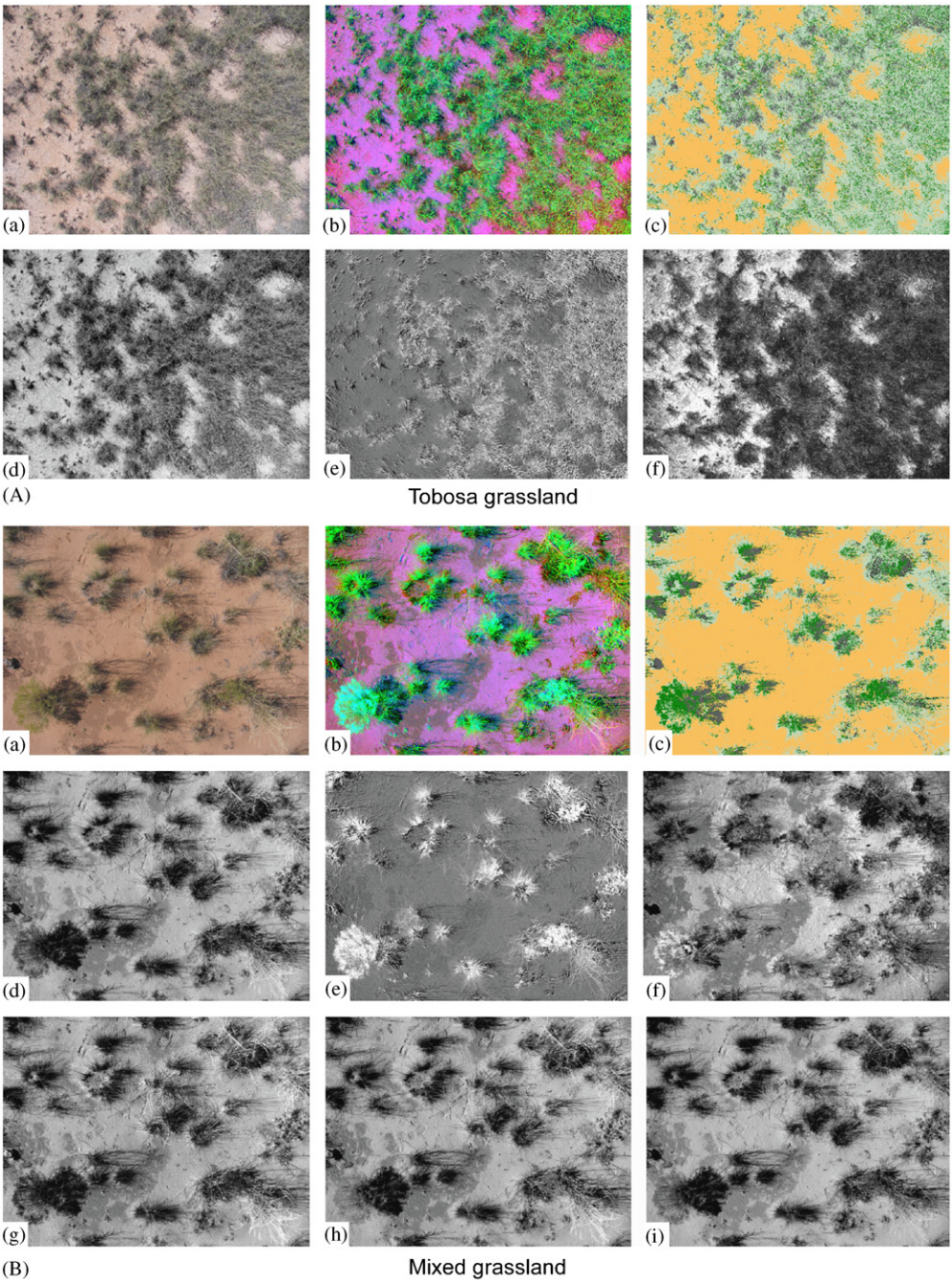

Fig. 3. Plot images of tobosa grassland (A) and mixed grassland (B). Shown are: 3-band images in RGB space (a), 3-band images in IHS space (b), classified images (c), and the following single bands: intensity (d), hue (e), saturation (f), and (for mixed grassland) blue (g), green (h), red (i). Classification colors in (c) represent *Soil* (yellow), *Shadow* (grey), *Green Vegetation* (dark green), and *Senescent Vegetation* (light green). Presentation resolution is 300 dpi (dots per inch).

Table 2
Correlation coefficients, *p*-values, estimates of mean differences and confidence intervals for comparisons of percent cover value estimates obtained from image analysis and line-point-intercept sampling

Type of cover	Correlation coefficient	*p*-value from paired *t*-test	Mean difference (% cover)	95% Confidence interval (% cover)
Total vegetation cover	0.9556	0.0002	−5.09	−7.56–−2.62
Soil	0.9391	0.2936	−1.46	−4.16–1.24
Green vegetation	0.8803	0.6975	−0.14	−0.87–0.58
Senescent vegetation	0.9523	0.0003	−4.94	−7.46–−2.43

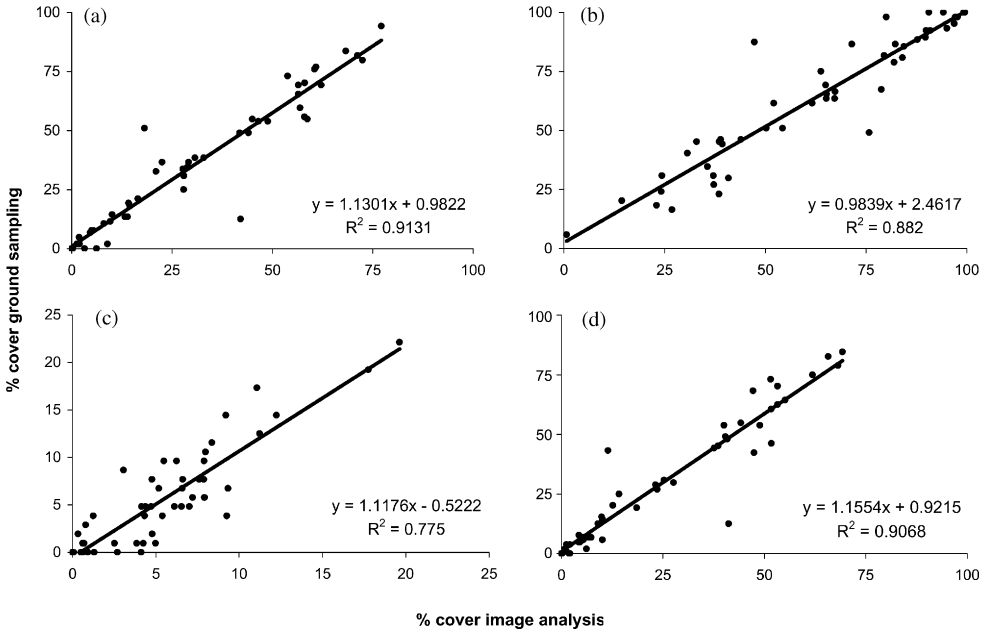

Fig. 4. Scatterplots for percent cover estimates of 50, 2.5 m × 3.5 m plots using object-based image analysis acquired 2.8 m above the soil surface of each plot and a line-point-intercept method using 4, 2.5 m lines within each plot to assess total vegetation cover (a), soil (b), green vegetation (c), and senescent vegetation (d).

image analysis underestimated total vegetation cover and senescent vegetation cover by approximately 5%, while no statistical differences in the mean differences between image analysis and LPI data were found for soil and green vegetation (using a paired *t*-test). The coefficient of variation (CV) was similar for total vegetation, bare soil and senescent vegetation indicating a similar level of precision for the image analysis and the LPI methods for these parameters (Table 3). However, LPI measurements generated a higher CV for green vegetation, suggesting that image-based analyses may be more effective where it is important to distinguish live from dead foliage in the top canopy layer.

Two outlier plots were detected in the graphs for total vegetation cover, soil and senescent vegetation (Fig. 4). Both outlier plots greatly differed in values for total cover, soil and senescent vegetation (i.e., 47% total cover from image analysis, 87% from ground

Table 3
Average parameter value and coefficient of variation based on image and line-point-intercept measurements (% cover)

	Average		Coefficient of variation	
Type of cover	Image	Ground	Image	Ground
Total vegetation cover	31.5	36.6	75.2	76.6
Soil	61.9	63.4	43.3	44.3
Green vegetation	5.7	5.8	74.2	91.9
Senescent vegetation	25.9	30.8	86.3	88.0

Table 4
Time requirements in hours for sampling and analyzing 50 plots for fractional cover with an image-based and line-point-intercept-based approach

	Field work	Office work	Total
Image-based	5.0[a]	12.9[b]	17.9
Ground-based	33.3[c]	3.0	36.3

Travel time between plots is not included.
[a]Based on 2 persons at 3 min/plot.
[b]Based on 1 person at 15.5 min/image.
[c]Based on 2 persons at 20 min/plot.

sampling for one of the plots), and we suspected that those two plots measured on the ground may not have been located in the exact position as the image taken of the plot.

In terms of labor and time involvement, the image-based method required slightly less than half the time required for the LPI method (Table 4). We did not take into account travel time between plots, which would be the same for ground sampling or image acquisition. Times for each plot were averaged. The time consuming part of ground sampling is the fieldwork, specifically setting up and measuring the plots, and it usually requires two people. It is possible for one person to conduct LPI sampling, which reduces field time, but this is often offset by increased fatigue and potentially reduced data quality associated with simultaneously reading and recording data.

For the image-based method, computer analysis required the most time. In our study, we used two people to acquire the images and record information, but one person could perform this task, reducing the total time to 15.4 h.

4. Discussion

This study showed that object-based image analysis using IHS-transformed images is a viable approach for estimating total cover of vegetation, bare soil, and fractional components of green and senescent vegetation using very high resolution ground photography. As others have found, IHS transformation can be very effective for analyzing vegetation in digital images (Ewing and Horton, 1999; Tang et al., 2000; Hemming and Rath, 2001). What set our study apart from previous studies was the use of object-based classification software, which offered more choices in features,

simple routines for masking and the combination of rule-based and nearest-neighbor classification.

The intensity, hue and saturation bands were less correlated than the red, green and blue bands and showed less overlap in the feature space for vegetation classification. We used the intensity band to mask shadows, which presents a common problem in ground photography. The saturation and hue bands were effective for separating soil and vegetation, so that green and senescent vegetation could be classified last in order to minimize the confusion of senescent vegetation with bright soil areas.

The object-based image analysis approach was also useful because it eliminated the "salt and pepper effect" common in pixel-based analysis of very high-resolution images. Adjacent areas of similar vegetation were automatically merged in the segmentation process. Partial automation of the image analysis process through use of protocols in eCognition was helpful in reducing time spent on each image. Manual fine-tuning of threshold values for shadow and soil was straightforward and, except for a few outliers, values did not differ much between images. We hope to increase the level of automation further as new versions of the software are released.

Correlations between image-based and LPI-based estimates of cover were relatively high, ranging from 0.88 to 0.96. We did not detect statistical differences in the estimates for soil and green vegetation. Booth et al. (2005) found that image analysis using the program VegMeasure (Johnson et al., 2003) estimated less green cover than estimates based on a 100-point laser frame at two study sites and obtained similar estimates at another site. Those authors attributed the discrepancies to limited, scattered green growth. In our plots, green vegetation was limited, scattered, and often mixed with senescent vegetation; and it appeared that the addition of the intensity, hue, and saturation bands was more effective than the use of the red, green and blue bands alone.

One of the difficulties in assessing whether image-based or ground-based estimates of fractional cover are more accurate is that we do not know the value of the true population. Booth et al. (2006) performed an experiment by using a poster of an image classification as a model of the true population and comparing it with several methods of ground-based percent cover estimates. The correlation coefficient of the model with LPI data in that study was 0.98. The size of the sampling point was given by Booth et al. (2006) as a 0.5 mm mark on a tape, while our pinpoint size was 1 mm. In addition, Booth et al. (2006) worked in a 2-dimensional system, while we were dealing with a 3-dimensional system. Therefore, direct comparisons of the correlations between LPI and image estimates are not possible, but have to be examined in context with the experimental setup.

It was expected that image analysis would overestimate cover because eCognition merges adjacent homogenous areas into image objects, including small spaces between plant canopy elements. LPI sampling does not include these spaces in its estimate of foliar cover. This error should decline as image resolution increases.

Our underestimation of total vegetation cover by approximately 5% can most likely be attributed to shadow influences. Shadow occurred both within the vegetation canopy, where it can be confused with dark green vegetation, as well as in the surrounding soil as shadow at the boundary of the plant canopy. Creating a separate class for shadow solved part of the problem, although we noticed that the discrepancies between percent cover values from ground and image-based analysis could mostly be attributed to shadow. Shadows can potentially be reduced or eliminated by shading the plot, which would improve the quality of the imagery (Booth et al., 2004), but would also increase costs.

Because our plot was larger than the 1 m^2 plots used by Booth et al. (2004), shading the plot would be more difficult and require additional workers. Another option would be to use a flash, although we are unsure how well this would work in intense light common to most deserts. Because our images were acquired during the last 2 weeks of October to coincide with a satellite overpass (the images were also used in another study), the sun angle was relatively low. If images can be acquired at times of the year with a higher sun angle, less shadow would be encountered. However, both forage value and canopy cover estimates are often required at various times throughout the year.

The image analysis method was less labor intensive and time consuming than the LPI method, and further labor saving could be achieved by only using one person for image acquisition. On the other hand, personnel require more experience with image analysis procedures. Our image analysis method using eCognition took more time for analysing each image (15 min) compared to using VegMeasure (1 min/image + 30–40 min for calibrating 25 images) in the study by Booth et al. (2005). The advantage of our technique is that the object-based segmentation approach has the ability to mask classes, and added flexibility when combining band means and ratios with membership functions in a fuzzy classification approach. In addition, other spectral, spatial, and contextual features can be included in these analyses. For a binary map output into vegetation and bare soil, the use of VegMeasure for image analysis of ground photos would be less time intensive. If, however, more classes and a larger number of features for the input bands are desired, the use of object-based image analysis is more appropriate. Our efforts will be directed at improving data flow and level of automation in image analysis, both of which will reduce cost.

Another improvement would be the addition of vegetation height information from remotely sensed data acquired with laser rangefinders or LiDAR (Light Detection and Ranging). Although our approach provided a good 2-dimensional view of canopy composition, 3-dimensional data would be even more informative for rangeland mapping, but also more costly.

Correlation coefficients between image- and LPI-based approaches are large enough to warrant further testing of this procedure as a remote sensing component of rangeland monitoring. The ground-based images could represent the finest scale in a series of multiscale images that tie ground-based rangeland measurements to landscape-scale assessments. Those linkages across spatial scales are important and can add a remote sensing component to the assessment of rangeland condition and trend (Herrick et al., 2006).

5. Conclusions

An image-based approach using object-oriented classification from very high resolution digital ground photography was an effective technique for estimating fractional cover of vegetation and soil and for separating green and senescent vegetation. This method showed high correlation with LPI data and required less time and labor than the LPI method. An added advantage is the establishment of permanent photographic plots that can be used to detect vegetation changes over time.

Points of consideration are the need for personnel with image analysis experience and software and hardware requirements for data flow and analysis, although once image analysis programs are purchased, they can be used for other purposes. We recommend

similar studies within differing vegetation communities to assess the effectiveness of this approach across an array of conditions. We hope to incorporate this approach in a multiscale image analysis study to pave the way for increased incorporation of remote sensing in rangeland monitoring and assessment.

Acknowledgements

The Jornada Experimental Range is administered by the USDA Agricultural Research Service, and is a National Science Foundation supported Long-Term Ecological Research Site (DEB 0080412). The authors thank Will Hooper for assistance with field data collection and Ericha Courtright for data analysis.

References

Bennett, L.T., Judd, T.S., Adams, M.A., 2000. Close-range vertical photography for measuring cover changes in perennial grasslands. Journal of Range Management 53, 634–641.

Bestelmeyer, B.T., Ward, J.P., Havstad, K.M., 2006. Soil-geomorphic heterogeneity governs patchy vegetation dynamics at an arid ecotone. Ecology 87, 963–973.

Booth, D.T., Cox, S.E., Louhaichi, M., Johnson, D.E., 2004. Lightweight camera stand for close-to-earth remote sensing. Journal of Range Management 57, 675–678.

Booth, D.T., Cox, S.E., Fifield, C., Phillips, M., Williamson, N., 2005. Image analysis compared with other methods for measuring ground cover. Arid Land Research and Management 19, 91–100.

Booth, D.T., Cox, S.E., Meikle, T.W., Fitzgerald, C., 2006. The accuracy of ground-cover measurements. Rangeland Ecology and Management 59, 179–188.

Burnett, C., Blaschke, T., 2003. A multi-scale segmentation/object relationship modelling methodology for landscape analysis. Ecological Modelling 168, 233–249.

Definiens, 2003. eCognition version 4.0.6 user guide, Definiens Imaging GmbH. Munich, Germany, pp. 486.

Ewing, R.P., Horton, R., 1999. Quantitative color image analysis of agronomic images. Agronomy Journal 91, 148–153.

Gibbens, R.P., McNeely, R.P., Havstad, K.M., Beck, R.F., Nolen, B., 2005. Vegetation changes in the Jornada Basin from 1858 to 1998. Journal of Arid Environments 61, 651–668.

Hay, G.J., Dube, P., Bouchard, A., Marceau, D.J., 2002. A scale-space primer for exploring and quantifying complex landscapes. Ecological Modelling 153, 27–49.

Hemming, J., Rath, T., 2001. Computer-vision-based weed identification under field conditions using controlled lighting. Journal of Agricultural Engineering Research 78, 233–243.

Herold, M., Liu, X., Clarke, K.C., 2003. Spatial metrics and image texture for mapping urban land use. Photogrammetric Engineering and Remote Sensing 69, 991–1001.

Herrick, J.E., Van Zee, J.W., Havstad, K.M., Burkett, L.M., Whitford, W.G., 2005. Monitoring Manual for Grassland, Shrubland and Savanna Ecosystems. USDA-ARS Jornada Experimental Range, Las Cruces, NM, pp. 236.

Herrick, J.E., Bestelmeyer, B.T., Archer, S., Tugel, A.J., Brown, J.R., 2006. An integrated framework for science-based arid land management. Journal of Arid Environments 65, 319–335.

Jensen, J.R., 2005. Introductory Digital Image Processing: a Remote Sensing Perspective, third ed. Prentice Hall, Upper Saddle River, NJ, pp. 164–167.

Johnson, D.E., Vulfson, M., Louhaichi, M., Harris, N.R., 2003. VegMeasure version 1.6 user's manual. Department of Rangeland Resources. Oregon State University, Corvallis, OR.

Karcher, D.E., Richardson, M.D., 2003. Quantifying turfgrass color using digital image analysis. Crop Science 43, 943–951.

Laliberte, A.S., Rango, A., Havstad, K.M., Paris, J.F., Beck, R.F., McNeely, R., Gonzalez, A.L., 2004. Object-oriented image analysis for mapping shrub encroachment from 1937–2003 in southern New Mexico. Remote Sensing of Environment 93, 198–210.

Laliberte, A.S., Fredrickson, E.L., Rango, A., Combining decision trees with hierarchical object-oriented image analysis for mapping arid rangelands. Photogrammetric Engineering and Remote Sensing, in press.

Leica Geosystems GIS and Mapping, 2003. Erdas Imagine 8.7 Field Guide. Leica Geosystems GIS and Mapping LLC, Atlanta, GA, pp. 698.

Lennartz, S.P., Congalton, R.G., 2004. Classifying and mapping forest cover types using Ikonos imagery in the northeastern United States. Proceedings of the ASPRS 2004 Annual Conference, Denver, CO, American Society for Photogrammetry and Remote Sensing, Bethesda, Maryland, unpaginated CDROM.

Louhaichi, M., Borman, M.M., Johnson, D.E., 2001. Spatially located platform and aerial photography for documentation of grazing impacts on wheat. Geocarto International 16, 63–68.

Okin, G.S., Gillette, D.A., Herrick, J.E., 2006. Multiscale controls on and consequences of aeolian processes in landscape change in arid and semiarid environments. Journal of Arid Environments 65, 253–275.

Richardson, M.D., Karcher, D.E., Purcell, L.C., 2001. Quantifying turfgrass cover using digital image analysis. Crop Science 41, 1884–1888.

Ryherd, S., Woodcock, C., 1996. Combining spectral and texture data in the segmentation of remotely sensed images. Photogrammetric Engineering and Remote Sensing 62, 181–194.

Tang, L., Tian, L., Steward, B.L., 2000. Color image segmentation with genetic algorithm for in-field weed sensing. Transactions of the American Society of Agricultural Engineers 43, 1019–1027.

Thomas, N., Hendrix, C., Congalton, R.G., 2003. A comparison of urban mapping methods using high-resolution digital imagery. Photogrammetric Engineering and Remote Sensing 69, 963–972.